Long distance beam propagation in colloidal suspensions: comparison between theory and experiment

E Wright, W Lee, P.-L Giscard, K Dholakia

Long distance beam propagation in colloidal suspensions: comparison between theory and experiment

E. M. Wright,[a, b] W. M. Lee[b], P.-L. Giscard[a] and K. Dholakia,[a, b]

[a] College of Optical Sciences, University of Arizona, Tucson, AZ85721

[b] SUPA, School of Physics and Astronomy, University of St Andrews, St Andrews, Fife KY16 9SS, United Kingdom

Abstract

It has been conjectured for some time that colloidal suspensions can act as artificial self-guiding media and support solitary beam-like solutions. The optical forces, along a diverging Gaussian beam, act to pull and retain the diffusing nanoparticles into its beam path. Consequently, the nanoparticle suspension acts to guide the diverging Gaussian beam and maintain the beam waist over a distance longer than its Rayleigh range. In this paper, we present a detailed analysis of beam propagation within nanoparticle suspensions. Using a recently developed theory by El-Ganainy *et. al.* (1), we seek to understand the beam dynamics by monitoring the scattered light from the particles along the propagation of the beam. An initial comparison of the theoretical and the experimental results shows interesting deviations due to the exponential nature of the optical nonlinearity.

Keywords: Nonlinear Optics, Solitons, optical trapping, nanoparticles

1. Introduction

Nonlinear optical processes have greatly enhanced our understanding of light matter interactions, and self-focusing of light beams in bulk media have maintained potential for applications in optical communications and optical waveguides. Self guiding of filaments for high peak power input beams propagating in transparent dielectric media (i.e. air, glass and water) has now become a mature field (2). In 1974 Bjorkholm and Ashkin (3) demonstrated the generation of an optical spatial soliton with sodium (atomic) vapour using a continuous-wave (cw) laser beam. They reported steady-state self-focusing, self-trapping, and self-defocusing of a cw laser beam in sodium vapor. With a mere 20-mW input power, they observed a self-trapped effect that resulted in a 12-cm-long filament with beam waist of 70 μm. Such a self-trapped effect essentially refers to the situation in which a propagating field maintains a relatively fixed beam profile of characteristic size w_o over an extended distance L.

To better understand this nonlinear optical mechanism, we may directly link it to the phenomenon of Kerr nonlinearity (2). In a Kerr-like medium, a Gaussian laser beam at low power (<critical power) would induce a refractive index profile proportional to its transverse intensity gradient thus resembling a convex lens. Due to diffraction, the beam would spread and as the result the intensity gradient would decay over the propagation direction. However, as one reaches the critical power, the refractive index of the Kerr medium would induce a nonlinear refractive-index profile such that the transverse intensity gradient is maintained over a much longer distance due to self-focusing and subsequent self-guiding. This sudden alteration is due the nonlinear dependence of the refractive index of the beam to the applied electric field of the light beam. In simple terms, a change of the local refractive index of the material equals to the present refractive index multiplied by the intensity. The self-trapped state is inherently unstable in an ideal three-dimensional Kerr medium. In two-dimensional systems, such as planar waveguides, self-trapped beams can be stable and lead to spatial optical solitons that resist diffraction. In some photorefractive medium i.e. strontium barium niobate crystals, there is sufficient scattering of the propagating field that one can use the scattered light to trace and monitor the beam profile (2).

Optical Trapping and Optical Micromanipulation V, edited by Kishan Dholakia, Gabriel C. Spalding,
Proc. of SPIE Vol. 7038, 70380P, (2008) · 0277-786X/08/$18 · doi: 10.1117/12.796243

The phenomenon of optical spatial solitons has been predicated and demonstrated in numerous media. Since discovering solitary waves in sodium vapor, Ashkin and co-workers (3-6) moved onto demonstrating such an effect in aqueous suspension of nanoparticles (colloidal nanosuspensions) with optical forces. Ashkin and co-workers were able to demonstrate some interesting nonlinear characteristics of the nanosuspension and vapor i.e. optical bistability (7) and self guiding (3) and four wave mixing (6). These experimental demonstrations showed that optical forces are a strong contributing factor in inducing a strong nonlinear response from colloidal nanosuspensions at relatively low average power (~1-2W). The colloidal nanosuspension can be treated as a form of photorefractive medium with each nanoparticle acting as a distinct single light scatter (point source). Hence, it would be possible to postulate that one can observe the evolution of the beam as it propagates into a colloidal medium by monitoring the scattered light (4, 8, 9).

In this paper, we revisit the work of Ashkin (4) and attempt to advance the understanding and simulation of the precise mechanism behind the nonlinear processes with a current theoretical model proposed out by R. El-Ganainy *et al* (1). We carry out our experiments using an optical fiber enclosed within a sealed capillary chamber. This allows us to fix the initial beam conditions of the experiments to enable us to try to match the theoretical predictions. The underlying physics of the nonlinearity is that electrostriction (gradient forces) pulls the nanoparticles into the regions of high intensity, assuming the nanoparticles have higher refractive index than the host liquid. The nanoparticles would then accumulate and result in a change of the local refractive index. As such, to lowest order the nanosuspension can be thought of as a Kerr-like medium where the change of the refractive index is dependent upon the intensity. In the case of the colloidal nanosuspensions, the Rayleigh scattering losses will also increase with the field intensity. The physical picture from the theoretical and experimental approach provides a qualitative picture that explains both our experiments and full simulations of long distance propagation in colloidal suspensions.

2. Theory

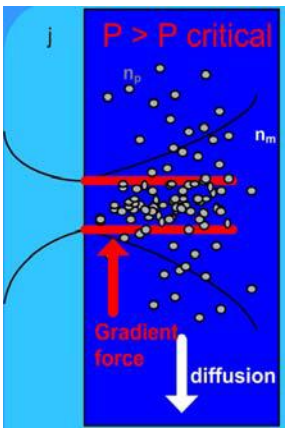

Figure.1 shows a schematic illustration of the system. A suspension of nanoparticles (gray circles) is being suspended in a aqueous solution of refractive index n_m. Upon reaching the critical power (P_{crit}), the gradient force acts to draw the diffusing nanoparticles into the highest intensity of the beam axis.

In Ref. (1) R. El-Ganainy *et al* proposed the theory where the gradient optical forces dominates the system and acts to pull particles towards the highest intensity of the input beam. In the initial steady state conditions, the particle drift is zero meaning that the particles that are moving into the beam equals to that of the particles diffusing out. The size of the nanoparticles used in this work needs to be approximate 10 to 20 smaller than the wavelength of the laser. At this size regime, the scattering cross section of these nanoparticles would be low and the gradient force would take govern over the particle motion. In the Rayleigh regime, the object may be considered as a point dipole and the contributions of the time-averaged gradient force $F_{gradient}$ and scattering forces $F_{scattering}$ may be readily separated as follows:

$$F_{gradient} = \frac{2\pi\alpha}{cn_m^{\ 2}}\nabla I \qquad (1)$$

$$F_{scattering} = \frac{I\sigma n_m}{c} \qquad (2)$$

where α denotes the polarisability of the sphere which for a standard non-absorbing dielectric object is proportional to the volume of the particle is equal to $n_m^2 r^3\left(\frac{m^2-1}{m^2+2}\right)$, σ is the scattering cross section of the sphere equal to $\frac{128\pi^5 r^6}{3\lambda^4}\left(\frac{m^2-1}{m^2+2}\right)^2$, r is the particle radius, I is the intensity, n_m is the refractive index of the surrounding medium, c denotes the speed of light, m refers to the ratio of the refractive indices of particle (n_p) to that of the surrounding medium (n_m) and λ is the wavelength of the trapping laser used. We can see from this that the scattering force is directly proportional to the trapping laser intensity and the gradient (or dipole) force upon the object is due to the inhomogeneous field gradient.

According to Ref. ((1), when a beam is introduced into the sample, as shown in figure.1, the volume filling factor of the particles within the beam given by $f(I)$ is related the intensity of the beam I by an exponential terms given by

$$f(I) = f_o e^{(\frac{\alpha}{4k_B t}I)} \qquad (3)$$

where k_B is Boltzmann constant and T is the temperature. The effective refractive index (nonlinear) is in turn directly related to the volume filling of the particles within the beam.

$$n_{eff}^2 = n_h^2(1+2f(I)\frac{n_s^2-n_h^2}{2n_h}) \qquad (4)$$

where the local refractive index is depend on n_{eff} is the effective refractive index, n_p and n_h are the refractive-indices of the colloidal spheres and host liquid. By incorporating the particle drift with respect to the gradient force into the Nerst-Planck equation, R. El-Ganainy *et al* (1) were able to develop a beam propagation model starting from the wave equation where the beam propagation incorporates the nonlinear refractive index dependence. In the current work, we also incorporate the intensity dependent volume filling factor (density) equation (3) into a paraxial wave equation for the electric field envelope $\varphi(r,z)$ which is written as

$$i\frac{\partial\varphi}{\partial z} + \frac{i}{2k_o n_b}\left[\frac{\partial^2}{\partial r^2} + \frac{1}{r}\frac{\partial}{\partial r}\right]\varphi + k_o(n_p - n_m)V_p f_o e^{(\frac{\alpha}{4k_B T}|\varphi|^2)} + \frac{i}{2}\sigma V_o f_o e^{(\frac{\alpha}{4k_B T}|\varphi|^2)} = 0 \qquad (5)$$

where z is the axial coordinate distance, r is the radial coordinate, $k_o = \frac{2\pi}{\lambda_o}$ is the wave number of the electric field.

In this equation (5), the first term describes beam propagation along the z-axis, the second term describes beam diffraction, and the third and fourth terms describe nonlinear refraction and Rayleigh scattering losses due to the nanosuspension, both of these terms having an exponential dependence on the propagation beam intensity $|\varphi|^2$. The model of El-Ganainy et al (1) therefore extends well beyond the usual Kerr model of self-focusing at high enough intensity. We have performed simulations based on this model for an initial Gaussian beam to compare with our experiments and that will be reported in the following pages.

3. Experiment

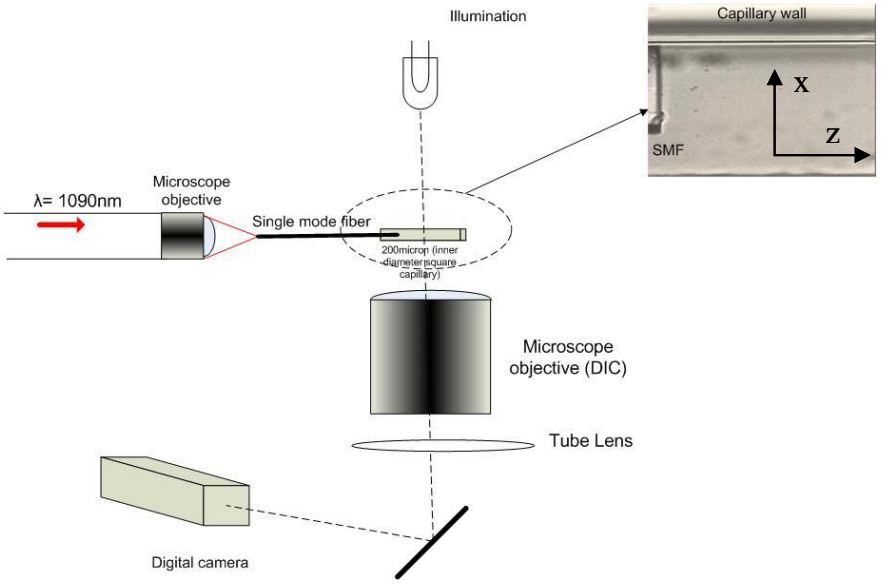

Figure.2 shows a schematic illustration of the experimental setup.

Many of the previous experiments (4, 8, 10) were carried using free-space coupling of the beam into the nanosuspension solution. The main drawbacks with focusing a free space laser into a sample are spherical aberration due to refractive index changes, beam pointing fluctuations, laser stability, and determination of the exact location of the beam waist. Spherical aberration arises from the fact that the light beam travels through two media of different refractive indices. The refractive index change would have a tendency of broadening the beam in the axial plane. This aberration effect would possibly create a larger focal region than before. In our work, the accurate knowledge of the beam waist entering into the sample is crucial to the observation of the beam dynamics so as to allow comparison with the theory. Beam pointing fluctuations and laser stability are inherent issues with free space due to fluctuations in the surrounding air medium. As the light beam of a fixed beam waist (air) enters into a medium of higher refractive index (water), the beam waist would have reduced due to the increase in refractive index. Many of these issues can be succumbed by the use of a single mode optical fiber. A single mode optical fiber provides the perfect beam launching platform. A laser (10W, 1090nm, SPI laser) is coupled into a single mode fiber (1060XP, Thorlabs, mode field diameter to 6.8 μm) using a three positioning fiber coupling stage (MDE122, Elliot scientific). The output end of the fiber is inserted into a capillary of inner diameter of 200 μm (VWR international). The sample is mounted onto an X-Y translations stage (H117, Prior Scientific) within an inverted microscope platform (TE2000E, Nikon). A 20X, NA 0.50 NA DIC (differential interferential contrast) microscope objective (Nikon) is used to image the sample onto a high speed digital camera (A622f Basler). During the initial single image acquisition, the high granularity present in the system creates a huge amount of intensity fluctuations. We circumvent this issue by using a frame averaging and points averaging technique. With the averaged data, we are able to collect a relatively smooth signal (~10-20% variations) from the Rayleigh scattered light from the nanoparticles. The nanoparticles used here are of (10% variation) hydrophobic polystyrene plain spheres of 0.099 μm in diameter (PS02N/6391, Bangs Lab). The initial concentration is $1.921 \text{ X } 10^{14}$particles/cm^3.

The averaging procedure has a second purpose. In the detection scheme our assumption is that each individual Rayleigh particle (0.099μm diameter) would scatter light uniformly in all directions. Hence, their scattered signal would indicate their current position. Analysis of the scattered light is through a series of frame-averaged images over a period of time (30s-60s). If a particle is randomly fluctuating within the beam position, their scattered signal would effectively average out (blur). While those particles that stays at their current location over a measured period within the beam

would maintain their scattered signal. A way to test this assumption is to create a random flow within the sample such that no nanoparticles will accumulate even at high powers. In the current experiment, we make use of a particle concentration of 1.921 X 10^9 particles/cm^3. At this concentration, we were able to observe a reduction of any additional background Rayleigh scattering from freely diffusing particles (turbid medium). In our experiment, we make use of the thermally-induced convective flow to create this random flow. The absportion of near infrared wavelength (1090nm in our case) for deionized water (H_20) and heavy water (D_20) can differ by almost three orders of magnitude with the former being more absorbing. With such a high absorption factor (for H20), we are expecting a high convective flow within the sample. This would propel the particles into random position and thus averaging out their signals. On the other hand, with D_20, the absorption factor is much lower and therefore a much reduced convection flow would be expected. The nanoparticles in D_20 would then stay confined within the beam would maintain their position and subsequently enhancing their individual signals. In figure.3 we show the one-dimensional plot of the on-axis intensity variation at x=0 over the beam propagation distance of (z) 300 μm. In figure 3 (a), we show the experimental results achieved with the nanosuspension in H_20. Even though the power has be increased close to 900 milliwatts, the overall scattered signal would resemble the linear diffraction with the decay of the intensity over its Rayleigh range ($\frac{\pi w_o^2}{\lambda}$). In contrast, for the D_20 samples, the overall scattered signals suggest an indication of particles accumulating within the beam, thus indicating possible nonlinear self-focusing behavior. The background signal is the inherent background intensity which the averaging procedure produces when there is no input beam. Figure.4 shows the false color image of the experiment shown in figure.3b

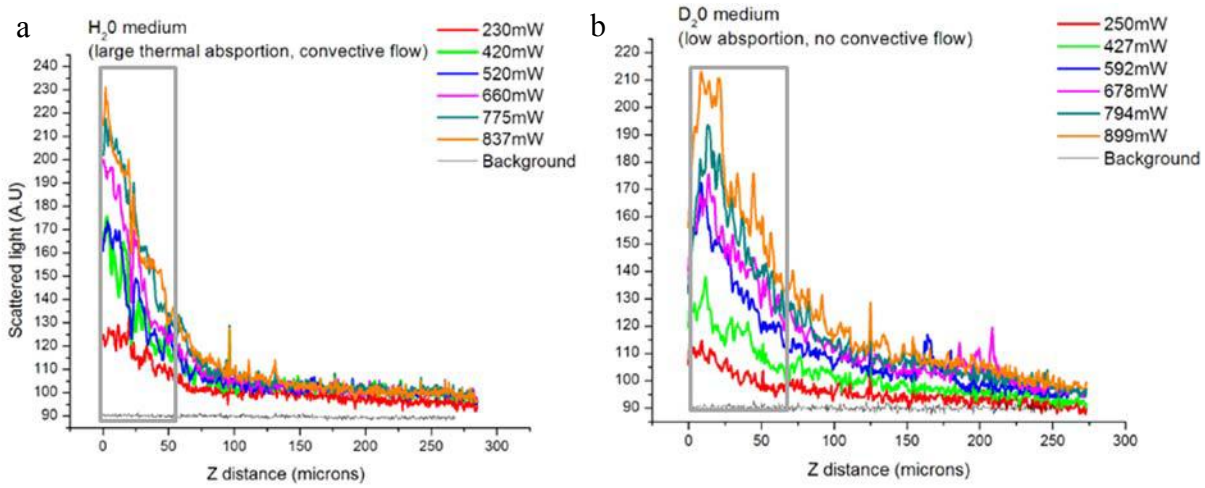

Figure 3 shows the light scattering from the nanosuspension (a) with and (b) without high levels of convective flow due to thermal absportion.

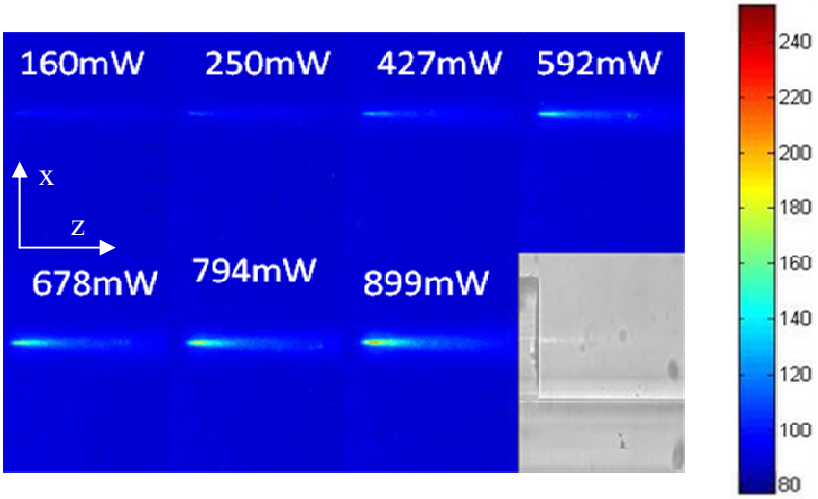

Figure 4 False colour images of the time-averaged scattered intensity from the nanosuspension.

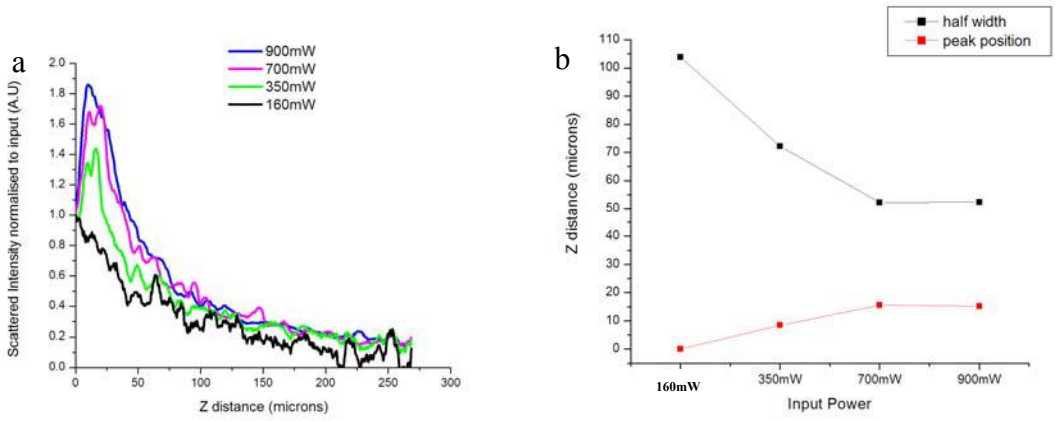

Figure 5 (a) Scattered light along the beam propagation direction (b) Half peak and peak position of the scattered light.

By normalizing the scattered light intensity to that at the input, as shown in figure 5a, we are able to look at the physical trends which the propagating field would exhibit through the scattered light. The two main trends that are evident are the change in the axial position along the z-axis of peak intensity and the axial position at which the on-axis intensity falls to half its value at the input, which we refer to as the half width. In figure 5b, we show that the half width decreases while the peak position of the colloids increases. This development in the peak intensity of the scattered light suggests that the nanoparticles are accumulating within beam. In some way, one can associate the accumulation of the particles with the excitation of a solitary wave, albeit an unstable solution. At the current concentration 1.921 X 10^{9} particles/cm^{3}, there exist too few particles (an average of 1.921X 10^{-3} particles/μm^{3}) to observe the extended formation of nanoparticles into a waveguide at the current power levels.. Thus we increased the concentration to 1.7 X 10^{13} particles/cm^{3} giving an average of ~17 particles/μm^{3}. This concentration does not obey the restrictions on the filling for the El-Ganainy theory to be valid (<3.7 X 10^{-4}) as one would need to include particle-particle interactions. However, experimentally it could allow us to observe solitary wave effects at lower powers. In figure.6, we show the linear alignment of nanoparticles viewed under differential interference contrast. The input power in this case is around 800 mW and the filling factor is 0.0086. The waveguide structure stretches for about 300 microns without any considerable change.

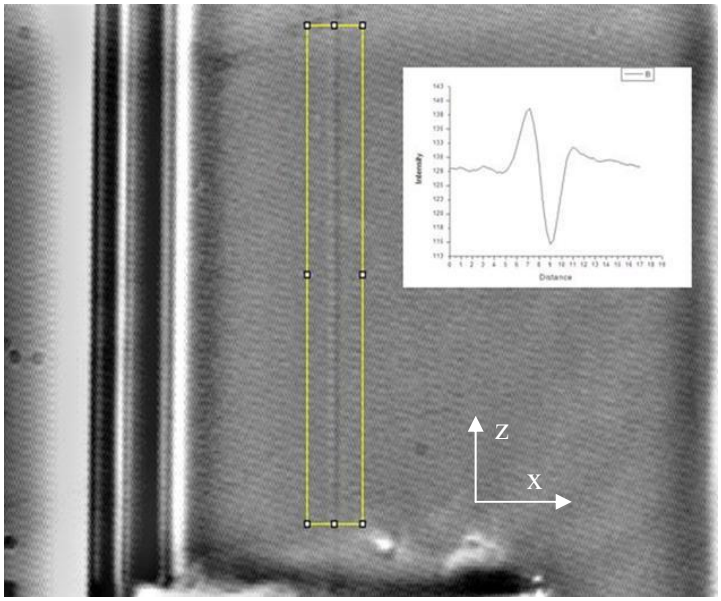

Figure 6 Formation of the polymer nanoparticles into a linear waveguide geometry viewed under differential interference contrast microscopy, as indicated by the yellow box. The inset shows the cross-section plot of the waveguide structure. Video 1. http://dx.doi.org/10. 1117/12.796243.1

4. Theory versus experiment

Next we look at the simulation results from the theoretical model and compare them to the current experimental results. The resolution of the simulation along the transverse grid is chosen to be 0.5 microns per grid point. The particle concentration is chosen is to be 1.921 X 10^9 particles/cm^3, the wavelength of laser beam , λ, in air is 1090nm and the beam waist, w_o, is chosen to be 3.4 μm. In figure.7, we show the simulation results (red) plotted against the experimental results (blue). The input power is varied from 0.25W to 0.794W. At the low powers, the light scattering is observed to follow the trend of linear diffraction. As seen in the simulation and experiment, figure.7a, the scattered light field as observed in the experiment reasonably matches that of the theoretical model. Here, there is no aggregation of particles along the beam light as such the scattering signal is not observed to increase. In the experiment, the increase in the input power (figure.7 b-e, 0.42W – 0.74W) seems to have a mark effect towards an increase in the scattered signal in the experiment. However, in the simulation, this effect is not observed for the range of input power. It was only an increase in the input in the simulation to 1.7W, when we start to see enhancement or increase in the scattering signal moving into the sample as seen in figure. 7f. Comparing figure.5 b and 7f, we can see a similar approach in which the scattered light varies experimentally and theoretically. In particular, we see that the axial position of the propagation beam maximum and the half width vary in a qualitatively similar manner in the theory and experiment. Furthermore, simulations of this based on a pure Kerr nonlinearity show that the position of peak intensity always occurs at z=0, so the movement of the peak intensity away from the input is therefore a key signature of the non-Kerr nature of the optical nonlinearity.

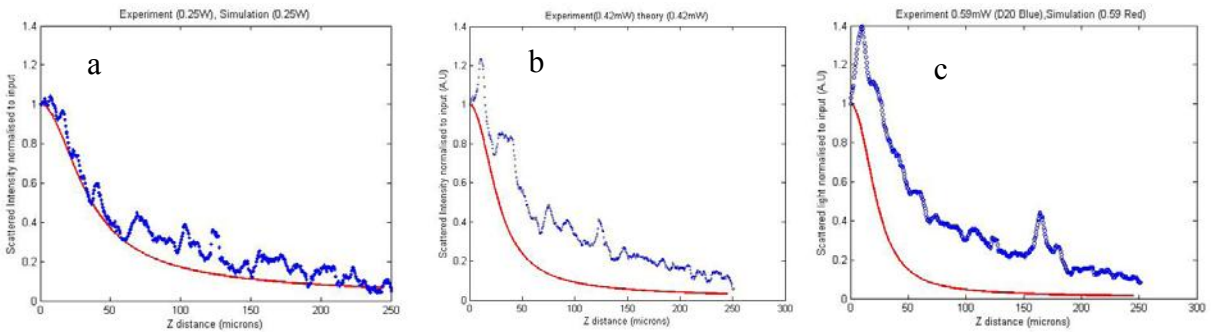

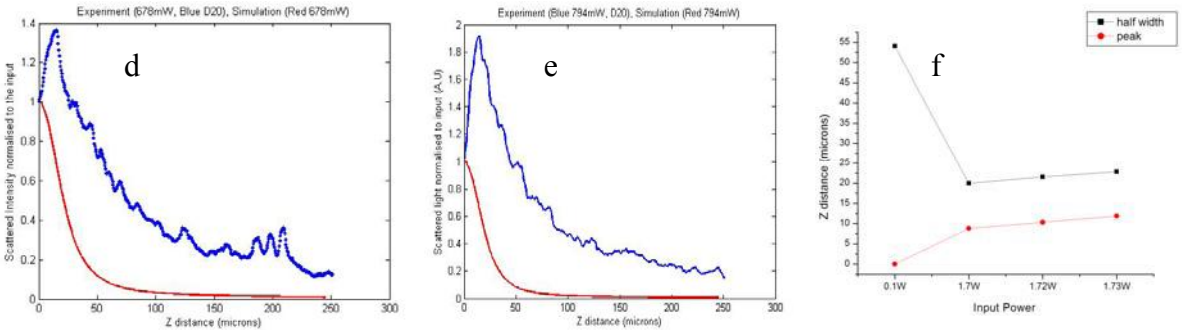

Figure 7 a-e. A series of comparison between the theory (red) and experimental results (blue) at different input powers. The intensities are normalised to the input. f shows the half peak and peak position of the intensity profile obtained theoretically.

5. Conclusion

The aim of this work was to compare the theoretical prediction and experimental result pertaining to the formation of solitary waves in nanosuspension. In our experimental work, we have observed, through the scattering light, the aggregation of nanoparticles along the beam as the input power is increased. Using two liquid media that have a large difference in their absorption, we were able to verify the accumulation of nanosuspension particles in the laser beam. With high random convective flow in the sample due to thermal effects, the scattering signal is seen to indicate no aggregation of colloids within the beam, while the solution with lower convective flow indicates that there is an aggregation of colloids within the beam. Next, we attempted to use a recent theory to model such the nonlinear effect. At the time of writing of this paper we have still not achieved detailed comparison between the El-Ganainy theory (1) and our experiment. This could be due to remaining issues in the experiment, eg. the use of the scattered light to monitor the beam propagation versus direct measurement of the beam intensity profile, or the need for including other physical effects in the model, eg. thermal effects and/or scattering forces. Even though, the theoretical model does indicate a similar trend towards the variations of the light scattering, the range of power required to reach that trend does not correlate well with the experiment.

6. Acknowledgement

The work is supported by funds from the UK Engineering and Physical Sciences Research Council. Ewan M. Wright is funded in part by the Joint Services Optical Program (JSOP). Kishan Dholakia is a Royal Society - Wolfson Merit Award holder.

References

1. R. El-Ganainy, D. N. Christodoulides, C. Rotschild and M. Segev, "Soliton dynamics and self-induced transparency in nonlinear nanosuspensions," *Opt. Express* 15(10207-10218 (2007)
2. G. I. Stegeman and M. Segev, "Optical Spatial Solitons and Their Interactions: Universality and Diversity," *Science* 286(5444), 1518-1523 (1999)
3. J. E. Bjorkholm and A. A. Ashkin, "cw Self-Focusing and Self-Trapping of Light in Sodium Vapor," *Physical Review Letters* 32(4), 129 (1974)
4. A. Ashkin, J. M. Dziedzic and P. W. Smith, "Continuous-wave self-focusing and self-trapping of light in artificial Kerr media," *Opt. Lett* 7(6), 276-278 (1982)
5. P. W. Smith, P. J. Maloney and A. Ashkin, "Use Of A Liquid Suspension Of Dielectric Spheres As An Artificial Kerr Medium," *Optics Letters* 7(8), 347-349 (1982)

6. P. W. Smith, A. Ashkin and W. J. Tomlinson, "4-Wave Mixing In An Artificial Kerr Medium," *Optics Letters* 6(6), 284-286 (1981)
7. P. W. Smith, A. Ashkin, J. E. Bjorkholm and D. J. Eilenberger, "Studies of self-focusing bistable devices using liquid suspensions of dielectric particles," *Opt. Lett* 9(4), 131 - 133 (1984)
8. V. E. Yashin, S. A. Chizhov, R. L. Sabirov, T. V. Starchikova, N. V. Vysotina, N. N. Rozanov, V. E. Semenov, V. A. Smirnov and S. V. Fedorov, "Formation of soliton-like light beams in an aqueous suspension of polystyrene particles " *Opt. Spectrosc.* 98(3), 511-514 (2005)
9. R. Sigel, G. Fytas, N. Vainos, S. Pispas and N. Hadjichristidis, "Pattern Formation in Homogeneous Polymer Solutions Induced by a Continuous-Wave Visible Laser," *Science* 297(5578), 67-70 (2002)
10. P. J. Reece, E. M. Wright and K. Dholakia, "Experimental observation of modulation instability and optical spatial soliton arrays in soft condensed matter " *Physical Review Letters* 98(20), 203902 (2007)